electronics

Article

Multi-Micro-Grid Main Body Electric Heating Double-Layer Sharing Strategy Based on Nash Game

Hui Wang [1,2,*], Chenglin Wang [1,2], Liang Zhao [3], Xiu Ji [1,2], Chengdong Yang [1,2] and Jiarui Wang [4]

[1] Changchun Institute of Technology, Changchun 130012, China
[2] National and Local Joint Engineering Research Center for Measurement, Control and Safe Operation of Intelligent Distribution Networks, Changchun 130012, China
[3] State Grid Jilin Electric Power Company, Changchun 130022, China
[4] State Grid JILIN Electric Power Research Institute, Changchun 130021, China
* Correspondence: sys3132022@163.com; Tel.: +86-13943054095

Abstract: In order to promote energy mutual aid among microgrids, expand the types of energy interaction, and improve the utilization of renewable energy, a two-layer sharing strategy for multi-microgrids (MMGs) based on the Nash game is proposed. Firstly, the low-carbon transformation of the micro-grid model is carried out, and the source side is transformed into a comprehensive and flexible operation mode for carbon capture thermal power plants. Then, the multi-microgrid subject electro-thermal double-layer sharing model based on the Nash game is constructed, which is decomposed into a revenue maximization sub-problem and a revenue redistribution sub-problem. In the sub-problem of revenue maximization, considering the lowest operation cost of carbon allowances and stepped carbon trading as the goal, the alternating direction multiplier method is used for a distributed solution. In the revenue redistribution sub-problem, the reasonable redistribution of income is realized by constructing the asymmetric energy mapping contribution function for different periods and energy types. Finally, the simulation results have verified the effectiveness of the proposed method. The results showed that the strategy of this paper can achieve the optimization of the economic objectives of the multi-microgrid (MMG) alliance and has the advantages of reasonable redistribution of benefits, promotion of wind and solar consumption, and reduction of carbon emissions.

Keywords: Nash game; multi-microgrids; electric-thermal bilevel sharing; P2G low-carbon transformation of thermal power plants; alternate direction multiplier method; CHP

Citation: Wang, H.; Wang, C.; Zhao, L.; Ji, X.; Yang, C.; Wang, J. Multi-Micro-Grid Main Body Electric Heating Double-Layer Sharing Strategy Based on Nash Game. *Electronics* **2023**, *12*, 214. https://doi.org/10.3390/electronics12010214

Academic Editor: Ali Mehrizi-Sani

Received: 22 November 2022
Revised: 23 December 2022
Accepted: 28 December 2022
Published: 1 January 2023

1. Introduction

The "China Research Report on Carbon Neutrality to 2060" pointed out: "Low-carbon and zero-carbon technologies are the key to achieving the goal of carbon neutrality, particularly in these aspects, such as the Capture, Utilization and Storage, CCUS), negative emissions and carbon sinks". To promote the efficient utilization of renewable energy and realize the low-carbon and clean energy supply of the power system [1], these will be one of the key research directions in the future.

A microgrid is an important way of aggregating producers and sellers. Internally, it contains various distributed power sources and multiple types of loads, which can promote the self-production and self-consumption of energy [2]. Meanwhile, externally, it can also interact with electrical grids to realize the energy supply and sales [3]. Peer-to-peer (P2P) energy trading among microgrids can effectively reduce the electricity cost of microgrids, improve the utilization rate of new energy and reduce carbon emissions [4].

The model of P2P energy trading among distributed multi-microgrid subjects can be divided into multiple directions, such as multi-agent [5], blockchain [6] and game theory [7–9]. This paper belongs to the game theory methods. In this category, the literature [10] was based on the Nash negotiation model to study the electricity transaction negotiation in the three main bodies of wind, photovoltaic and hydrogen. The main bodies of wind and solar energy act as two unidirectional supply sides, and the main body of electric hydrogen production is used as a one-way to the receiving demand side. The model of electric energy sharing transaction volume adopts the augmented Lagrange multiplier method, utilizing the benefit redistribution with the method of three-way equal sharing, which maximizes the benefits of the micro-grid alliance. Reference [11] studied the Nash negotiation problem of multi-microgrid power transaction in the power grid environment, which means the Nash bargaining method of the multi-microgrid power transaction is proposed and a cooperative game model is constructed. In references [12,13], they have tried to expand the interior of the multi-microgrid main body into an electrically coupled integrated energy system, build a multi-agent architecture of the integrated energy system and use game theory to optimize its scheduling, to achieve multi-agent collaborative optimal operation. In reference [14], considering the operation mechanism of carbon trading, the low-carbon transformation of cogeneration units in microgrid is carried out, and a multi-microgrid power sharing strategy based on asymmetric Nash negotiation is proposed. The simulation results showed that this strategy can effectively reduce carbon emissions in microgrids. While we can say that they have proposed the model of a more comprehensive multi-energy flow coupling relationship for the unsolvable issues, in References [15,16], the carbon capture power plant was reformed, and the absorption, storage, time shift and release of CO_2 were realized by introducing flue gas diversion and controlling solution concentration. The power consumption of carbon capture and utilization was transferred to the nighttime to promote the consumption of abandoned wind, so as to realize the dual-benefits of the economic and low-carbon way, and at the same time, the lower limit of the net output of thermal power units can be broadened to improve the spinning reserve. The operation mode is expanded, and the three-stage economic model of source-load is constructed to improve the problems of load loss and wind curtailment. In references [17–19], they have used game theory methods to model multi-microgrid entities from various perspectives, all of which have achieved significant results. Reference [20] evaluated different methods of galvanically isolated monitoring of the main voltage waveforms to determine the degree of distortion of the output signal relative to the input signal and the suitability of each method for calculating active power values. Reference [21] projected an event-triggered distributed hybrid control scheme for safe and economical operations. Reference [22] puts forward a multi-period and multi-energy operation model, where the power, heating and natural gas networks are coupled and managed through distributed energy hubs for multi-carrier energy systems. Reference [23] presented a two-stage mixed-integer linear programming method for regional-level multi-energy-system (MES) planning, considering distributed renewable energy integration based on the Energy-Hub (EH) model. Reference [24] introduced a distributed algorithm for the triggered event—with some desirable properties, namely distributed execution, asynchronous communication and independent computation.

The above studies have promoted the progress of multi-microgrid main energy sharing strategies, but they are all limited to a single type of electric energy sharing strategy and have not fully explored the sharing potential of multiple energy sources, such as the electric heat in multi-microgrids, which include cogeneration. The main research work of this paper differs from the existing work as follows: the flue gas shunt carbon capture and power-to-gas devices suitable for cogeneration are introduced to further carry out the electric-heat-gas-hydrogen-carbon coupling low-carbon transformation of the microgrid; furthermore, the type of energy interaction is expanded, especially for the power-only electric energy interaction among the multi-microgrid subject is extended to include electrothermal double-layer interaction, and the Nash game is used to solve the energy interaction quantity in a distributed manner. By constructing an asymmetric energy mapping contribution function of the supply and demand sides, time periods and energy types, the interests of the multi-microgrid alliance can be further reasonably redistributed. Finally, we have verified the effectiveness of the strategy by an example through studying multiple methods.

2. The Electric Heating Sharing Architecture in MMGs

In this paper, a multi-microgrid P2P electric heating energy sharing architecture based on the Internet of Things technology is constructed. As shown in Figure 1, each microgrid's main body has an independent electric heating energy exchange (microgrid energy trading, MET), and the microgrids use wireless networks for communication contact, such as 5G communication; their data are connected to external communication through MET and terminal collection and control facilities to realize P2P transactions. The software that completes the transaction function is called the Energy Trading System (ETS).

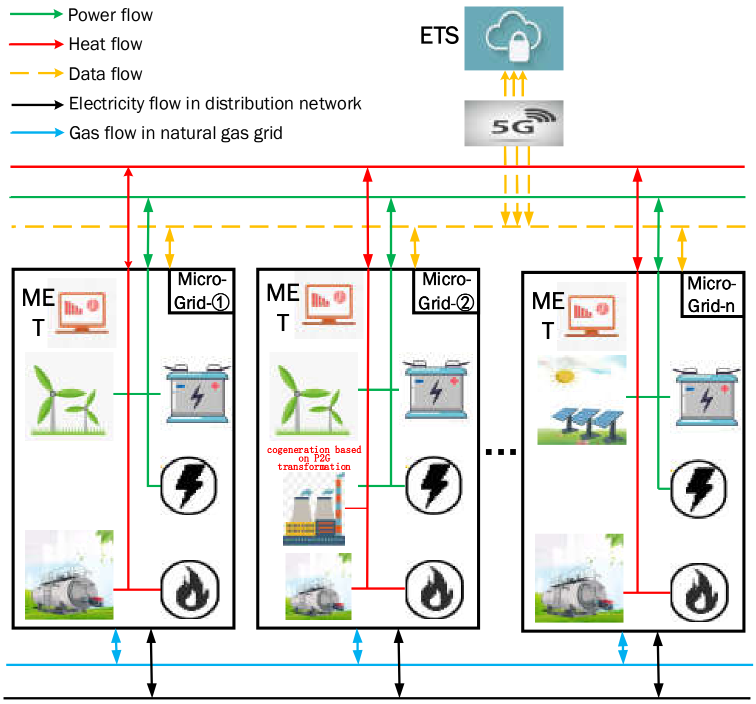

Figure 1. Multi-microgrid main P2P electric heating energy sharing architecture diagram.

3. The Independent Operation Model in Microgrids

Here, considering the cogeneration of electricity, heat and gas, the multi-energy flow synergy in micro-grids is studied. Due to the fact that the operation of the thermal-electric units in microgrids will generate a large amount of carbon dioxide, which does not meet the requirements of low-carbon, this paper will carry out a low-carbon transformation. As shown in Figure 2, flue gas diversion, liquid-storage carbon capture and storage, and methanation devices are introduced to complete the three-stage transformation of P2G. Considering the interaction with external power grids, gas grids and energy sharing among micro-grids, a low-carbon micro-grid architecture that introduces P2G and energy sharing is formed.

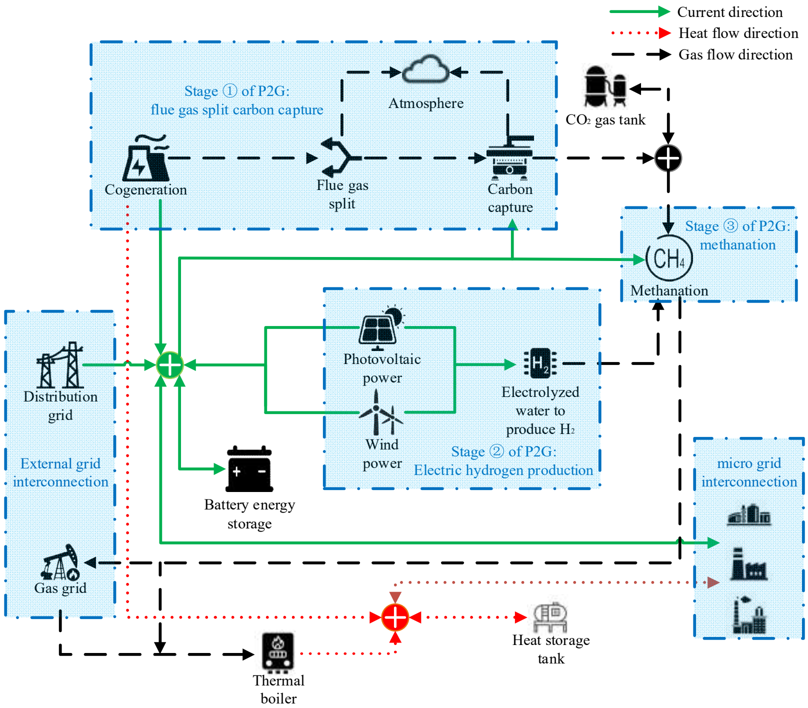

Figure 2. Low-carbon micro-grid architecture diagram introducing P2G and energy sharing.

3.1. The Lowest Operating Cost Model in the Independent Operation Mode of Micro-Grids

The objective function of the minimum operating cost of the micro-grid after the low-carbon transformation is as follows:

$$\begin{cases} W_{sum}^0 = \sum_{i=1}^N W_i^0 \\ W_i^0 = W_i^{YCL} + W_i^{WH} + W_i^{CO2} \end{cases}. \tag{1}$$

In the formula, W_{sum}^0 is the sum of the operation costs of all micro-grids under the independent operation mode; W_i^0 is the total operation cost of the micro-grid i; W_i^{YCL} is the raw material cost; W_i^{WH} is the maintenance cost; W_i^{CO2} is the carbon transaction cost; N is the number of multi-microgrid main bodies. Its sub-cost composition is as follows:

(1). Raw material cost

$$\begin{cases} W_i^{YCL} = W_i^M + W_i^{CH4} + W_i^E \\ W_i^M = \sum_{t=1}^T a_0 \cdot [a_1 (E_{i,t}^{CHP})^2 + a_2 E_{i,t}^{CHP} + a_3] \cdot \triangle t \\ W_i^{CH4} = \sum_{t=1}^T [pri\_g^{buy} G_{i,t}^{buy} - pri\_g^{sell} G_{i,t}^{sell}] \cdot \triangle t \\ W_i^E = \sum_{t=1}^T [pri\_e^{buy} E_{i,t}^{buy} - pri\_e^{sell} E_{i,t}^{sell}] \cdot \triangle t \end{cases}. \tag{2}$$

In the formula, W_i^M is the cost of natural gas; W_i^{CH4} is the cost of buying and selling natural gas; W_i^E is the cost of buying and selling electricity; a_0 is the cost per kilogram of coal; $E_{i,t}^{CHP}$ is the cogeneration output; a_1, a_2 *and* a_3 are the fitting coefficients of the quadratic linear relationship between coal consumption rate and thermo-electric power; pri_g^{buy} and pri_g^{sell} are the gas prices; $G_{i,t}^{buy}$ and $G_{i,t}^{sell}$ are the gas powers; pri_g^{buy} and pri_g^{sell} are the time-of-use electricity prices; $E_{i,t}^{buy}$ and $E_{i,t}^{sell}$ are the main network powers; $\triangle$t is the time scale value.

(2). Maintenance cost

$$\begin{cases} W_i^{WH} = W_i^{DG} + W_i^{BA} + W_i^{DR} \\ W_i^{DG} = \sum_{t=1}^{T} (d_1 E_{i,t}^{PV} + d_2 E_{i,t}^{Wind}) \\ W_i^{BA} = \sum_{t=1}^{T} (e_1 E_{i,t}^{BA,C} + e_2 E_{i,t}^{BA,Disc}) \\ W_i^{DR} = \sum_{t=1}^{T} (f_1 E_{i,t}^{cut} + f_2 E_{i,t}^{tran} + f_3 H_{i,t}^{tran}) \end{cases}. \quad (3)$$

In the formula, W_i^{WH} is the maintenance cost; W_i^{DG} is the cost of distributed power generation; W_i^{BA} is the battery depreciation cost; W_i^{DR} is the demand response cost; d_1 *and* d_2 are the unit electricity costs in the life cycle of the photovoltaic fan; $E_{i,t}^{Wind}$ and $E_{i,t}^{PV}$ are the wind turbine and photovoltaic, respectively; $e_1 e_2$ is the battery charge and discharge depreciation coefficient; $E_{i,t}^{BA,C}$ and $E_{i,t}^{BA,Disc}$ are the charge and discharge powers of the battery; f_1, f_2 and f_3 are the response compensation unit prices that can reduce the transferable electrical load and transferable thermal load; $E_{i,t}^{cut}$, $E_{i,t}^{tran}$ and $H_{i,t}^{tran}$ are the reduction of electrical load, transfer of electrical load and transfer of thermal load.

(3). Ladder carbon transaction cost

$$\begin{cases} T_i^{CO2} = C_i^{paifang} - C_i^{P2G} - C_i^{peie} \\ C_i^{paifang} = \sum_{t=1}^{T} (g_1 E_{i,t}^{CHP} + g_2 H_{i,t}^{CHP} + g_3 H_{i,t}^{GL}) \\ C_i^{peie} = \sum_{t=1}^{T} (l_1 E_i^{fa} + l_2 H_i^{fa}) \\ P_i^{fa} = \sum_{t=1}^{T} (E_{i,t}^{PV} + E_{i,t}^{Wind} + E_{i,t}^{CHP}) \\ H_i^{fa} = \sum_{t=1}^{T} (H_{i,t}^{CHP} + H_{i,t}^{GL}) \end{cases}. \quad (4)$$

In the formula, T_i^{CO2} is the carbon trading volume of the micro-grid; $C_i^{paifang}$ is the carbon emission volume; C_i^{P2G} is the carbon absorption volume; C_i^{peie} is the amount of carbon allowances; Carbon emission is related to power generation and heating power; g_1, g_2 *and* g_3 are the carbon emission coefficients; $E_{i,t}^{CHP}$, $H_{i,t}^{CHP}$ and $H_{i,t}^{GL}$ are the power generation and heat generation of CHP and heat boiler, respectively; the carbon emission quota is proportional to the power generation E_i^{fa} and the heat production H_i^{fa}. The proportional coefficients are the carbon quota coefficients l_1 *and* l_2. After obtaining the carbon emission trading volume, the carbon emission cost can be solved by solving the function according to the stepped positive and negative carbon trading volume:

$$W_i^{CO2} = \begin{cases} -\lambda l - \lambda(1+\alpha)l + \lambda(1+\alpha)^2(T_i^{CO2} + 2l) & T_i^{CO2} \le -2l \\ -\lambda l + \lambda(1+\alpha)(T_i^{CO2} + l) & -2l \le T_i^{CO2} \le -l \\ \lambda T_i^{CO2} & -l \le T_i^{CO2} \le 0 \\ \lambda T_i^{CO2} & 0 \le T_i^{CO2} \le l \\ \lambda l + \lambda(1+\alpha)(T_i^{CO2} - l) & l \le T_i^{CO2} \le 2l \\ \lambda l + \lambda(1+\alpha)l + \lambda(1+\alpha)^2(T_i^{CO2} - 2l) & T_i^{CO2} \ge 2l \end{cases} \quad (5)$$

In the formula, W_i^{CO2} is the stepped carbon transaction cost; λ is the base price of carbon trading; l is the length of the carbon emission interval; $1+\alpha$ is the price growth rate.

The solution of the minimum cost objective function needs to be solved on the basis of the following system electric and heat balance constraints and modeling constraints of key equipment. The electrical power balance constraints are as follows:

$$E_{i,t}^{CHPe1} - E_{i,t}^{CCS} - E_{i,t}^{P2G} + E_{i,t}^{buy} + E_{i,t}^{PV} + E_{i,t}^{Wind} + E_{i,t}^{BADisc} = E_{i,t}^{sell} + E_{i,t}^{load} + E_{i,t}^{BAC} \quad (6)$$

In the formula, $E_{i,t}^{CHPe1}$ is the net output of the cogeneration unit; $E_{i,t}^{CCS}$ is the carbon capture power consumption; $E_{i,t}^{P2G}$ is the electricity-to-gas power consumption; $E_{i,t}^{load}$ is the electrical load after demand response; the thermal power balance constraints are as follows:

$$H_{i,t}^{CHP} + H_{i,t}^{GL} = H_{i,t}^{load}. \quad (7)$$

In the formula, $H_{i,t}^{load}$ is the heat load after the demand response.

3.2. P2G Three-Stage Refined Model with CHP

The following introduces the P2G three-step refinement model of cogeneration flue gas diversion carbon capture.

Based on the framework of Figure 2, a three-stage refined model of P2G for comprehensively excavating wind and light abandonment to produce hydrogen and flue gas split-flow carbon capture is proposed, as follows:

(1). Stage ①: Flue gas split-flow carbon capture.

The thermoelectric coupling output constraints of traditional cogeneration are as follows:

$$\begin{cases} E_t^{CHP} \geq \max\{E_{\min}^{CHP} - k_{\min}H_t^{CHP}, k_l(H_t^{CHP} - H_0^{CHP})\} \\ E_t^{CHP} \leq E_{\max}^{CHP} - k_{\max}H_t^{CHP} \\ H_t^{CHP} \geq 0 \\ H_{i,t}^{GB} = V_{i,t}^{GB}\eta_{GB}Q_{CH_4} \end{cases} \tag{8}$$

In the formula, E_t^{CHP} is the total power output of CHP; $E_{\min}^{CHP}$ is the total minimum power output of CHP; H_0^{CHP} is the heat production power when the power generation is the smallest; $E_{\max}^{CHP}$ is the total maximum power output of CHP; H_t^{CHP} is the heat generation power at time t; $k_{\min}$ and $k_{\max}$ are the limit of lower and upper slope of the electric-thermal coupling constraints, and the electric-thermal ratio at the maximum coal utilization rate; $H_{i,t}^{GB}$ is the heat production power of the gas boiler; $V_{i,t}^{GB}$ is the natural gas consumption of the gas boiler; η_{GB} is the heat production efficiency of flue gas boiler; Q_{CH_4} is the combustion heat value of natural gas.

A large amount of carbon is emitted during the operation of cogeneration, which can be sequestered by carbon capture after the flue gas diversion. As a cheap carbon source in the first stage of power-to-gas conversion, its operation model is as follows:

$$C_{i,t}^{CCS} = \chi \cdot (C_{i,t}^{HD} + C_{i,t}^{MT}) \cdot \varepsilon \tag{9}$$

In the formula, $C_{i,t}^{CCS}$ is the carbon capture power of micro-grid i at time t; χ is the flue gas split ratio; ε is the carbon capture efficiency; $C_{i,t}^{HD}$ and $C_{i,t}^{MT}$ are the carbon emissions of thermal power plants and micro-combustion turbines.

(2). Stage ②: Electro-hydrogen production.

In order to avoid the generation of additional CO_2 in the hydrogen production stage of P2G, the electricity source of electric hydrogen production in this paper can be only clean energy, such as wind and photovoltaic power. In this paper, the waste electricity of clean energy sources such as wind and photovoltaics is preferentially used to produce hydrogen, so as to avoid the energy consumption of electricity for hydrogen production to generate additional CO_2. Additionally, the operating model constraints are as follows:

$$\begin{cases} H_{i,t}^{EL} = U_{EL} \cdot f(\frac{E_{i,t}^{EL}}{E_{rated}^{EL}}) \cdot H_{rated}^{EL} \\ O_{i,t}^{EL} = \upsilon \cdot H_{i,t}^{EL} \\ f(\frac{E_{i,t}^{EL}}{E_{rated}^{EL}}) = \mathrm{a}_{EL}(\frac{E_{i,t}^{EL}}{E_{rated}^{EL}})^2 + \mathrm{b}_{EL}(\frac{E_{i,t}^{EL}}{E_{rated}^{EL}}) + c_{EL} \\ E_{i,t}^{EL} \leq E_{i,t}^{Wind} + E_{i,t}^{PV} \\ U_{EL} \cdot E_{\min}^{EL} \leq E_{i,t}^{EL} \leq U_{EL} \cdot E_{\max}^{EL} \end{cases}. \tag{10}$$

In the formula, $H_{i,t}^{EL}$, H_{rated}^{EL} and $O_{i,t}^{EL}$ are the real-time power, rated power and real-time power of the electrolyzer to produce hydrogen, respectively; υ is the power ratio of producing oxygen and hydrogen; U_{EL} is the identification bit of electrolytic cell switch status; $E_{i,t}^{EL}$, E_{rated}^{EL}, E_{min}^{EL} and E_{max}^{EL} are the real-time, rated, minimum and maximum power consumption of electrolytic cell electrolyzer, respectively; a_{EL}, b_{EL} and c_{EL} are the coefficients of the electrolyzer efficiency function, respectively, where $c_{EL} = 1 - a_{EL} - b_{EL}$; $E_{i,t}^{Wind}$ and $E_{i,t}^{PV}$ are the fan and photovoltaic power, respectively.

(3). Stage ③: Synthesis of methane from hydrogen and carbon dioxide.

The cheap hydrogen produced by abandoning the wind and light and the CO_2 captured by the carbon capture after the flue gas shunting can synthesize natural gas with high stability, which can be directly supplied to the thermal boiler to generate heat* or to the gas load in the area, or imported into the natural gas pipeline for remote operation. For distance transmission, the electrical coupling constraints are as follows:

$$\begin{cases} C_{i,t}^{P2G} = \kappa_1 \cdot G_{i,t}^{G} \\ H_{i,t}^{P2G} = \kappa_2 \cdot G_{i,t}^{G} \\ E_{i,t}^{P2G} = \kappa_3 \cdot G_{i,t}^{G} \\ G_{\min}^{G} \le G_{i,t}^{G} \le G_{\max}^{G} \end{cases} \tag{11}$$

In the formula, $C_{i,t}^{P2G}$ is the carbon consumption power of the electric-to-gas device of micro-grid i at time t; $G_{i,t}^{G}$ is the power of methane generated by the electric-to-gas device of micro-grid i at time t; κ_1, κ_2 and κ_3 are the ratios of methane to carbon dioxide, hydrogen, oxygen and power consumption during the operation of the methanation unit, respectively; $G_{\max}^{G}$ and $G_{\min}^{G}$ are the upper and lower limits of the power to generate methane, respectively.

4. Electric Heating Double-Layer Sharing Model Based on Nash Game

The Nash game is a kind of cooperative game, which is often used to deal with market competition. The Nash game model needs to satisfy a set of axioms, and the solution and the product maximization is the equilibrium solution of the Nash game problem [16].

The following Formula (13) is the standard model for the Nash game to deal with the sharing of electricity and heat among the subjects of multiple micro-grids:

$$\begin{cases} max\prod_{i=1}^{N} \left(W_i^0 - W_i^{EHP2P}\right) \\ s.t. W_i^0 \ge W_i^{EHP2P}, \text{formula } (2) - (11) \end{cases} . \tag{12}$$

In the formula, W_i^0 is the maximum individual benefit when the micro-grid i operates in isolation, that is, the operating cost at the breakdown point of negotiation; W_i^{EHP2P} is the operating cost of the micro-grid alliance after supporting the sharing of electric heating energy; Formulas (2)–(12) is the constraint condition.

The established Nash game model (14) is a non-convex non-linear optimization problem, which is very difficult to solve directly. It is decomposed into the sub-problem P of maximizing the benefits of each micro-grid main body's electric-thermal interaction alliance and the sub-problem Q of the reasonable redistribution of alliance interests, and the optimal solution of model (14) can be obtained by solving them in turn.

4.1. Solving the Sub-Problem P of Alliance Revenue Maximization

The purpose of the sub-problem P of maximizing the revenue of the multi-microgrid subject alliance is to obtain the electric and thermal interaction between the micro-grid's main body when the alliance's profit is maximized. Due to the fact that the Alternating Direction Method of Multipliers (ADMM) algorithm has the advantages of good convergence characteristics, a simple form and strong robustness, it is often used to solve such optimization problems with separable variables.

Considering the long distance between micro-grids, whether it is the transmission of electric energy through the large power grid or the transmission of thermal energy through the self-built network, investment costs or network costs are required. Therefore, the electricity and heat interaction costs between micro-grids are considered in this paper.

$W_{i\to j}^{P2P}$, the electricity and heat interactive transmission cost of the micro-grid i, can be calculated as follows:

$$W_i^{ep2p} = \sum_{j=1}^{N}\sum_{t=1}^{T}\left(m_{i\to j}^{P2P}\left|E_{i-j,t}^{P2P}\right|\right), j \neq i\ , \tag{13}$$

$$W_i^{hp2p} = \sum_{j=1}^{N}\sum_{t=1}^{T}\left(M_{i\to j}^{P2P}\left|H_{i-j,t}^{P2P}\right|\right), j \neq i\ . \tag{14}$$

In the formula, W_i^{ep2p} and W_i^{hp2p} are the total cost of electricity and thermal energy transmission that microgrid i needs to pay for the interaction with other micro-grids; $m_{i\to j}^{P2P}$ and $M_{i\to j}^{P2P}$ are the transmission costs of the unit electric energy and the unit heat energy from micro-grid i to micro-grid j at time t; E_{i-j}^{P2P} is the electric power transmitted from micro-grid i to micro-grid j at time t; H_{i-j}^{P2P} is the transmission cost of micro-grid i to micro-grid thermal power of micro-grid j.

4.1.1. Solution of the Sub-Problem P1 of Electricity Sharing in the Lower Layer of the Alliance

After introducing the variable of electricity sharing transactions between micro-grids, its output value will dynamically change with the electricity balance equation affected by the energy interaction, although the output constraint interval of each device does not change. The new electrical balance equation of each micro-grid in the system is changed from Formula (6) to the following:

$$E_{i,t}^{CHPe1} - E_{i,t}^{CCS} - E_{i,t}^{P2G} + E_{i,t}^{buy} + E_{i,t}^{DG} + E_{i,t}^{BADisc} = E_{i,t}^{sell} + E_{i,t}^{load} + E_{i,t}^{BAC} + \sum_{j=1,j\neq i}^{N} E_{i\to j,t}^{P2P} \tag{15}$$

In the formula, $E_{i,t}^{CHPe1}$ is the net output of the cogeneration unit; $E_{i,t}^{CCS}$ is the carbon capture power consumption; $E_{i,t}^{P2G}$ is the electricity-to-gas power consumption; $E_{i,t}^{buy}$ and $E_{i,t}^{sell}$ are the buying and selling electric power of the main network; $E_{i,t}^{BA,C}$ and $E_{i,t}^{BA,Disc}$ are the charging and discharging power of the battery, respectively; $E_{i,t}^{load}$ is the electric load after the demand response; $E_{i\to j,t}^{P2P}$ is the electric power shared by micro-grid i to micro-grid j. $E_{i,t}^{DG}$ is the sum of the electrical output of all distributed power sources in the micro-grid i at time t.

Then, after considering electricity sharing, the total operating cost of the alliance will also change from Equation (1) to:

$$\begin{cases} W_{sum}^{EP2P} = \sum_{i=1}^{N} W_i^{EP2P} \\ W_i^{EP2P} = W_i^{YCL} + W_i^{WH} + W_i^{CO2} + W_i^{ep2p} \end{cases} . \tag{16}$$

In the formula, W_{sum}^{EP2P} is the sum of the multi-microgrid operating costs after the end of the first stage of electricity sharing, and W_i^{EP2P} represents the operating cost of the i-micro-grid after electricity sharing.

According to the principle of the alternating direction multiplier method, the sub-problem of maximizing the benefit of the alliance can be transformed into the problem of minimizing the total operating cost after the alliance [10]:

$$\begin{cases} min\sum_{i=1}^{N} W_i^{EP2P}(E_{i\to 1}^{P2P}, E_{i\to 2}^{P2P}, \cdots, E_{i\to j}^{P2P}, \cdots, E_{i\to N}^{P2P}), j \neq i, j \in [1, N] \\ s.t. E_{i\to j}^{P2P} + E_{j\to i}^{P2P} = 0, j \neq i, i \in [1, N], j \in [1, N] \end{cases} . \tag{17}$$

Then, the specific steps of distributed solution based on the ADMM algorithm are as follows:

(1). Construct the augmented LaGrangian multiplier structure of the objective function of the minimum operating cost of the alliance, as follows:

$$\begin{cases} L_n^{P1} = \sum_{i=1}^{N} W_i^{EP2P} + \sum_{k=1}^{N\cdot(N-1)} \left[\lambda_k^n (E_{i\to j}^{P2P} + E_{j\to i}^{P2P}) + \frac{\rho}{2} \cdot \| E_{i\to j}^{P2P} + E_{j\to i}^{P2P} \|_2^2 \right] \\ n \le n_{\max} \end{cases} . \quad (18)$$

In the formula, L_n^{P1} is the sum of the augmented costs of the first-stage electronic sharing sub-problem of multiple micro-grids in the nth generation; λ_k^n is the LaGrange multiplier, and k is the unique number corresponding to the combination of e micro-grid i and micro-grid j; set the penalty constant of the augmentation term $\rho = 10^{-4}$; n is the current number of iterations, and the maximum value is n_{max}; the initialization iteration number is 1, and the transaction volume of power sharing between multi-micro-grids is initialized to 0 and the Lagrange multiplier is initialized to 0.

(2). The Formula (18) decomposed into a distributed iterative solution model (19) of each micro-grid. There are $2(N-1)$ interaction quantities E_{i-j}^{p2p} in each micro-grid, and N-1 augmentation LaGrange multiplier λ_k^{n}.

$$\begin{cases} L_{n,i}^{P1} = W_i^{MG} + \sum_{j=1}^{N} \left[\lambda_k^n (E_{i\to j}^{P2P} + E_{j\to i}^{P2P}) + \frac{\rho}{2} \cdot \| E_{i\to j}^{P2P} + E_{j\to i}^{P2P} \|_2^2 \right] \\ \text{st } (2)-(5), (7)-(11), (15) \end{cases} \quad (19)$$

In the formula, $L_{n,i}^{P1}$ is the sum of the augmented cost of the electronic sharing subproblem in the nth generation of the micro-grid i in the first stage.

(3). The electric energy sharing transaction variables are iteratively updated according to Formula (19) and (20) until all $2N$ $(N-1)$ electric energy interaction variables are updated.

$$E_{i\to j}^{P2P,n+1} = \text{argmin}_{E_{i\to j}^{P2P}} L_{n,i}^{P1} \quad (20)$$

(4). According to the electricity sharing transaction volume between the new generation of micro-grids, it is brought into Formula (21) to iteratively update all N $(N-1)$ LaGrangian multipliers λ_k^{n+1}.

$$\lambda_k^{n+1} = \lambda_k^n + \rho(E_{i\to j}^{P2P,n+1} + E_{j\to i}^{P2P,n+1}) . \quad (21)$$

(5). Update the number of iterations n.

$$nn + 1. \quad (22)$$

(6). Determine whether the current objective function has converged.

$$\begin{cases} \sum_{t=1}^{T} \sum_{i=1}^{N} \sum_{j=1}^{N} \| E_{t,i\to j}^{P2P,n+1} + E_{t,j\to i}^{P2P,n+1} \|_2^2 \le \varsigma^{\text{Consensuality}} \\ \sum_{t=1}^{T} \sum_{i=1}^{N} \sum_{j=1}^{N} \| E_{t,i\to j}^{P2P,n+1} - E_{t,i\to j}^{P2P,n} \|_2^2 \le \varsigma^{\text{Convergence}} \\ orn \ge n_{\max} \end{cases} . \quad (23)$$

In the formula, $\varsigma^{\text{Consensuality}}$ is the consensus convergence factor, and $\varsigma^{\text{Convergence}}$ is the complementary convergence factor.

The iteration will terminate if the above equation is satisfied. Otherwise, return to (20)–(22) to enter the next iteration until the convergence condition is satisfied or the set maximum number of iterations $n_{\max}$ is reached.

So far, the electric energy interaction $E_{i-j}^{P2P,end}$ of the sub-problem P1 with the lowest operating cost of the alliance and the new operating cost $W_i^{P2P,end}$ of each micro-grid subject after the alliance are solved. By substituting $W_i^{P2P,end}$ into Formula (16) to obtain the lowest total running cost $W_{sum}^{P2P,end}$ after the alliance.

4.1.2. Solution of Sub-Problem P2 in the Upper-Layer Heat Sharing in Multi-Microgrid

After the solution of the lower-layer electricity sharing sub-problem P1 is completed, the constant value of the electricity sharing transaction volume $E_{i-j}^{P2P,end}$ can be obtained, which is brought into the individual operation cost objective function W_i^0 of Formula (6) to update W_i^0. Then, a new shared thermal energy transaction constant $Price^{P2P,H}$ between 0 and the lowest heat production cost is added. Then, with reference to sub-problem P1, the E_{i-j}^{P2P} in each step is replaced by H_{i-j}^{P2P}, and the iterative solution is obtained. The constant value of the thermal energy sharing transaction volume $H_{i-j}^{P2P,end}$ and the running cost $W_{sum}^{P2P,end}$ after the double-layer sharing of electric and heating can be further reduced.

So far, the optimal transaction volume of electricity and heat sharing among multi-micro-grid subjects has been fully solved. In order to further improve the sharing satisfaction, it is often necessary to redistribute benefits [16].

4.2. Solving Sub-Problem Q of Redistribution of Alliance Income

The benefit redistribution is mainly to redistribute the benefit after the coalition revenue maximization sub-problems P1 and P2 are solved, and the reduction of the total operating cost of the alliance compared with the total operating cost of the isolated multi-microgrid. The reduction formula is:

$$W^D = \sum_{i=1}^{N} W_i^0 - \sum_{i=1}^{N} W_i^{EHP2P,end} . \tag{24}$$

In the formula, W^D is the reduction amount.

Benefit redistribution is based on the respective contributions of all individuals and considers the two types of energy distributions: time-of-use electricity price, electric energy and thermal energy. The contribution function is constructed as follows:

$$\begin{cases} \theta_i = \theta_i^E + \theta_i^H \\ \theta_i^E = \sum_{t=1}^{T} (pri\_e_t^{buy} E_{i,t}^{P2P,s} - pri\_e_t^{sell} E_{i,t}^{P2P,b}) \\ \theta_i^H = \sum_{t=1}^{T} (pri\_h_t^{buy} H_{i,t}^{P2P,s} - pri\_h_t^{sell} H_{i,t}^{P2P,b}) \end{cases} \tag{25}$$

In the formula: θ_i is the initial contribution of micro-grid i; θ_i^E and θ_i^H are the contribution of electricity and heat transaction of micro-grid i, respectively; pri_g^{buy} and pri_g^{sell} are the gas prices for buying and selling, respectively; $pri\_e_t{}^{buy}$ and $pri\_e_t{}^{sell}$ are the time-of-use electricity prices; $pri\_h_t{}^{buy}$ and $pri\_h_t{}^{sell}$ are the heat prices for gas buying and selling, respectively; $E_{i,t}^{P2P,S}$ is the sum of electricity sold from micro-grid i to all other micro-grids at time t; $E_{i,t}^{P2P,b}$ is the electricity purchased from micro-grid i to all other microgrids at time t. The $H_{i,t}^{P2P,S}$ is the sum of the heat that microgrid i sells to all other micro-grids at time t; $H_{i,t}^{P2P,b}$ is the sum of the heat that micro-grid i buys to all other micro-grids at time t.

In order to further stimulate the energy interaction, the linearly increasing contribution can be mapped to an exponential increase. In order to avoid the excessive power series, normalization can be further performed. The final contribution of each micro-network subject is:

$$\tau_i = e^{\frac{\theta_i}{\sum_{i=1}^{N} \theta_i}} - 1 . \tag{26}$$

In the formula: τ is the final contribution degree of micro-grid i.

So far, only according to the proportion of the contribution of each micro-grid to the total contribution of the multi-micro-grid, the increased benefits of the multi-microgrid alliance in the sub-problem P are allocated proportionally:

$$w_i^{EHP2P} = \frac{\tau_i}{\sum_{i=1}^{N} \tau_i} W^D . \tag{27}$$

In the formula, w_i^{EHP2P} is the redistribution benefit value obtained by micro-grid *i* in sub-problem Q.

$$W_i^{0EHP2P} = W_i^0 - W_i^{EHP2P}. \tag{28}$$

The final actual total operation cost W_i^{0EHPEP} of microgrid i after participating in P2P electric heating energy sharing can be obtained by taking the difference between the negotiation breakpoint cost and the redistribution value of cooperative alliance income, finally.

5. Example Analysis

The example in this paper uses the CPLEX plug-in of MATLAB software for simulation analysis.

5.1. Calculation Parameters

The case study in this paper considers the *P2P* electric heating energy sharing transaction problem among the three micro-grids. Figure 3a–c are the main base source-load curves of micro-grids ①, ② and ③, respectively; Figure 3d is the fluctuation curve of the purchase and sale price of electricity in one day. Micro-grids ① and ③ are the wind-solar-electric field micro-grids in a certain place, and micro-grid ② is a low-carbon micro-grid improved by introducing P2G. The photovoltaic wind power and electric heating load data are typical daily data in a certain area. The setting of micro-grid parameters can reflect the contradiction between supply and demand of different sources and loads in each micro-grid. In order to enhance the orderliness of energy interaction among multiple agents, the different unit interaction costs are set among micro-grid individuals. The parameters of the calculation example are shown in Appendix A, and the basic source-load curve of each micro-grid main body is shown in Figure 3.

5.2. Analysis of Operating Results of Individual Low-Carbon Transformations of Micro-Grids

As an example, this paper presents a comparative analysis of the results before and after the introduction of P2G into the micro-grid for low-carbon transformation. Figure 4a,b below are the electric power diagram and the carbon power diagram for the low-carbon operation of micro-grid ② with the introduction of P2G.

As can be seen from Figure 4, the green line identifies the electrical power, and the black line identifies the carbon power; in micro-grid ②, due to the relatively large capacity of the electric load relative to the wind turbine, the wind power always runs in the maximum power of the tracking state, and the shortfall is supplemented by the cogeneration power generation. Cogeneration power generation has less power generation in the valley electricity price period, and the priority is to consume the wind power preferentially. During the peak electricity price period, the combined heat and power generation generates 6000 kW at full power and realizes the profit of selling power to the large power grids. The carbon capture equipment operates at its maximum limit power of 1000 kW during the flat valley electricity price period to achieve maximum carbon capture. The daily carbon capture CO_2 is converted into natural gas during the valley period, and the power consumption is 646.28 kW, which is less than the power conversion limit of 1000 kW. With a limit of 1000 kW, it can be found that, due to the existence of CO_2 solution storage, the carbon capture power can be decoupled from the methanation power, which can further increase the system's flexibility and economy.

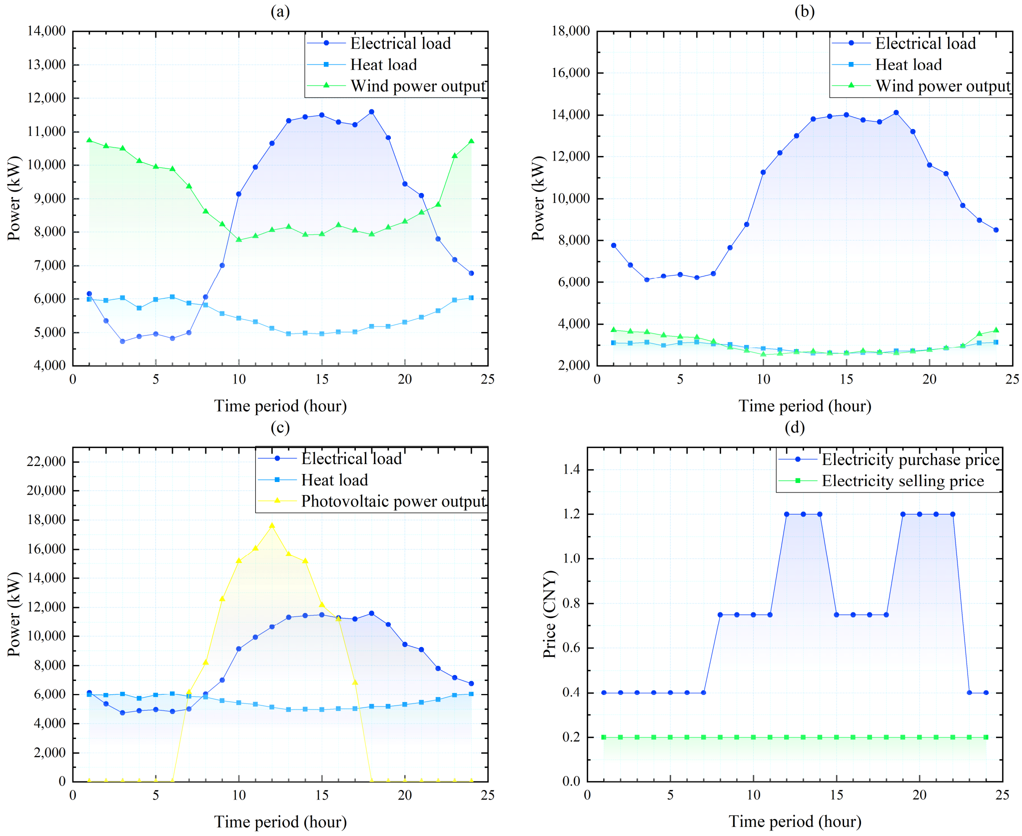

Figure 3. Basic source−load curves of the main bodies of each micro−grid. (**a**) Source−load curves of micro−grid ①. (**b**) Source−load curves of micro−grid ②. (**c**) Source−load curves of micro−grid ③. (**d**) Electricity purchase and selling price of distribution grid.

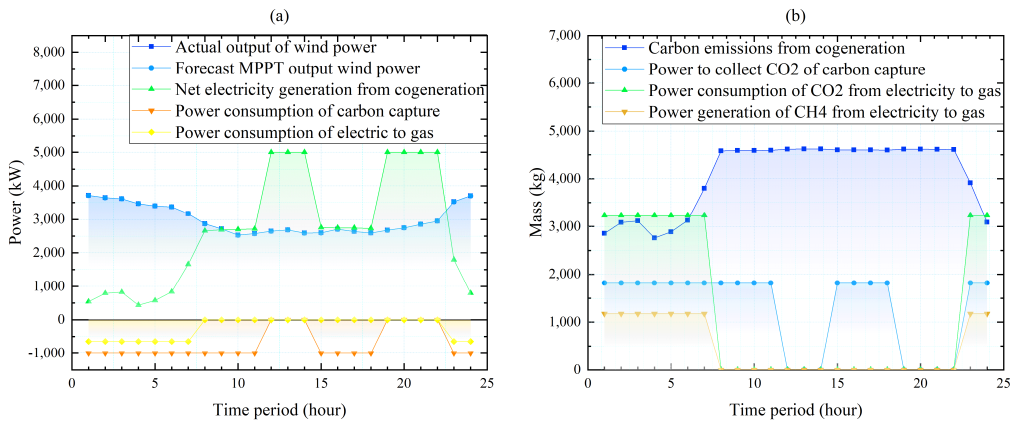

Figure 4. Micro−grid 2 introduces P2G low−carbon operation electric carbon power. (**a**) Electric power of micro−grid 2. (**b**) Carbon power of micro−grid 2.

Appendix A is a comparative analysis table before and after the introduction of P2G for micro-grid 2 for low-carbon transformation. Before the transformation, the actual carbon emission was 95,223 kg, the carbon transaction cost was 6176 CNY and the total operating cost was 64,717 CNY. After the transformation, the introduced P2G can carry out the carbon capture and methanation of CO_2, consume 43,885 kg, and the actual carbon emission is reduced to 68,457 kg, which is optimized by 28.1% compared with that before the transformation. The carbon transaction cost is 4248 CNY, a decrease of 31.2 percent; the total operating cost of the system is 63,055 CNY, which is reduced by 2.6%. It can be seen that carbon emissions, carbon transaction costs and total operating costs have been reduced to varying degrees after the transformation of individual micro-grids.

5.3. Analysis of the Sub-Problem P of the Benefit Maximization of MMGs Based on the Nash Game

In this paper, the Nash game is used to solve the lower-layer electric energy interaction quantum problem P1 and the upper-layer thermal energy interaction quantum problem P2 of energy sharing in the multi-micro-grid alliance. It is necessary to analyze the convergence and optimality of the operation cost of the electric and thermal double-layer distributed iterative solution, the complementarity of the energy interaction between the main bodies of the microgrid, and the consumption of abandoned wind and light, as well as the daily dispatching output and electric-thermal balance results of each equipment in the system analyzed.

5.3.1. Convergence Analysis Based on Nash Game

On the basis of the operation cost of the negotiation breaking point of the independent operation of each micro-grid in the previous section, this section verifies the correctness and superiority of the distributed solution of the electric and thermal double-layer sharing between the main bodies of the micro-grid by introducing the Nash game.

Figure 5a–c are the iterative results of the operating costs of the micro-grids ①, ② and ③ for the electricity sharing P1 sub-problem, respectively. Figure 6a–c are the iterative results of the running costs of the micro-grids ①, ② and ③ for the heat sharing P2 sub-problem, respectively. Figures 5d and 6d are the iterative results of the alliance running cost, relying on a personal computer to solve mixed integer linearization. After only 26 iterations and 15 iterations, respectively, the flatness is achieved, and the time spent is less than five minutes, which proves the efficient convergence of the distributed solution.

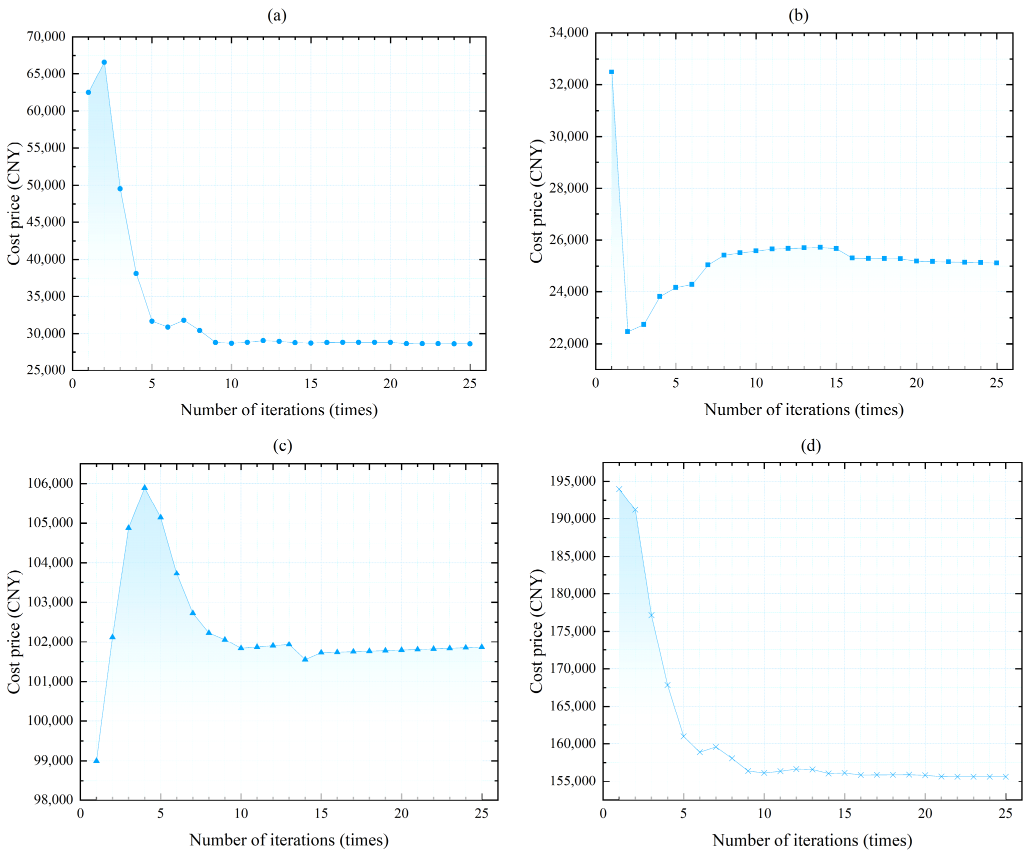

Figure 5. Convergence results of the coalition total running cost of the sub−problem P1 of the lower−level electricity sharing. (**a**) Iterative result of the micro−grid ①. (**b**) Iterative result of the micro−grid ②. (**c**) Iterative result of the micro−grid ③. (**d**) Iterated results of the alliance costs.

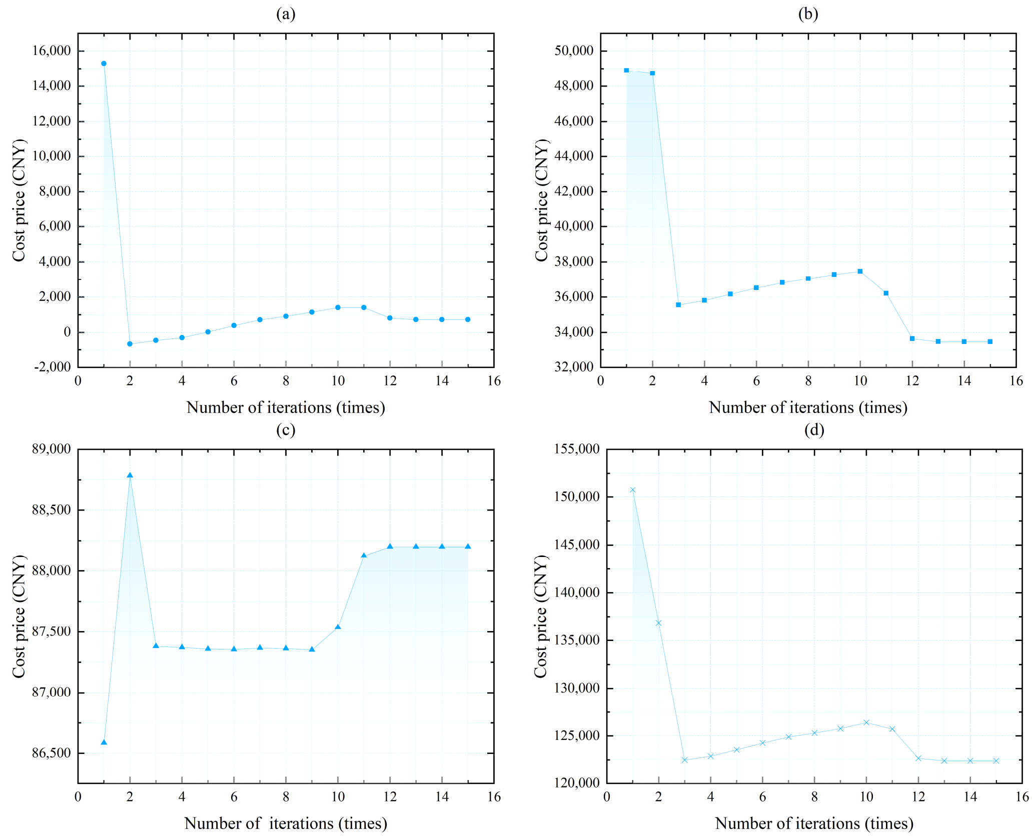

Figure 6. Convergence result of the coalition total running cost for upper-layer hot-sharing sub−problem P2. (**a**) Iterative result of the micro−grid ①. (**b**) Iterative result of the micro−grid ②. (**c**) Iterative result of the micro−grid ③. (**d**) Iterated results of the alliance costs.

At the same time, the lower-level electronic sharing sub-problem P1 optimizes the total operating cost of the alliance from 193,320 CNY at the negotiation breaking point to 155,641 CNY; the upper-level heat-sharing sub-problem P2 can continue to iteratively optimize the total alliance operating cost to 122,395 CNY. The effectiveness of the distributed optimization algorithm based on the Nash game is proposed effectively in this paper.

5.3.2. The Analysis of the Results of Complementarity and Abandoned Wind and Solar Energy Consumption

Due to the fact that the iterative solution of the Nash game is an approximate solution with small errors, it is necessary to verify the complementarity of the energy interaction between micro-grids in Formula (1), as shown in Figure 7:

It can be seen from the interaction results of electricity sharing in the lower layer of Figure 7a that at any time, the electric and thermal interactive power of micro-grids ①, ② and ③ is balanced; between the times of 1–9 and 20–24, the curtailed wind power of micro-grid ① is transmitted to micro-grids ② and ③ for use, and the abandoned light of micro-grid ③ is transmitted to micro-grids ① and ② for use at 8–15 moments. It shows that the power sharing between micro-grids improves the consumption of wind and light and reduces the power purchase of the main network of the alliance, which is more economical.

As shown in Figure 7b, in this example, there are cogeneration units in micro-grid ②, which is used as a heat source to share heat energy, with micro-grids ① and ③ as heat loads; the heat energy is shared from micro-grid ② to micro-grid ① and micro-grid ③. At any time, the thermal energy interaction power balance of micro-grids ①, ② and ③ reduces the heating cost.

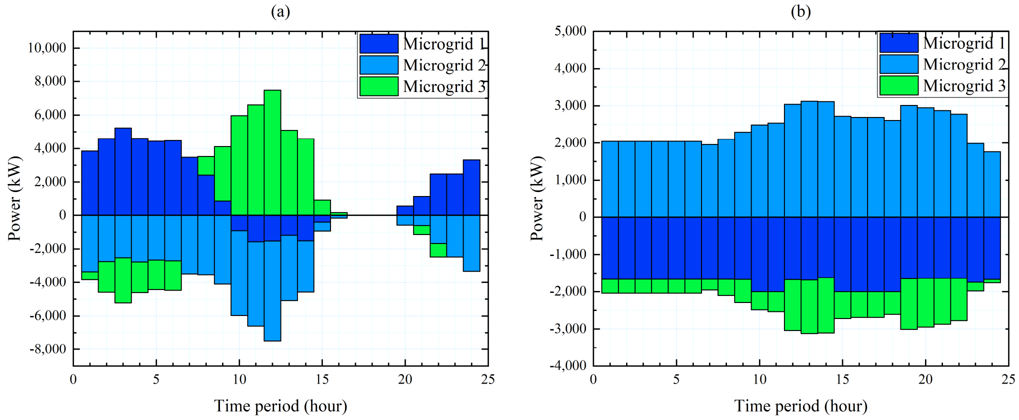

Figure 7. The results of energy interaction between micro−grids. (**a**) Electric interaction results. (**b**) Heat interaction results.

5.3.3. The Analysis of Daily Dispatch Output and Electric-Heat Balance Results

Figure 8a,b are the electric power balance and thermal power balance in micro-grid ② after the electric heating double-layer sharing solution, respectively. The positive and negative half-axes are all electrothermal outputs, and the negative half-axes are all electrical and thermal loads. The positive and negative half-axes are symmetrical to verify the electrical and thermal balance.

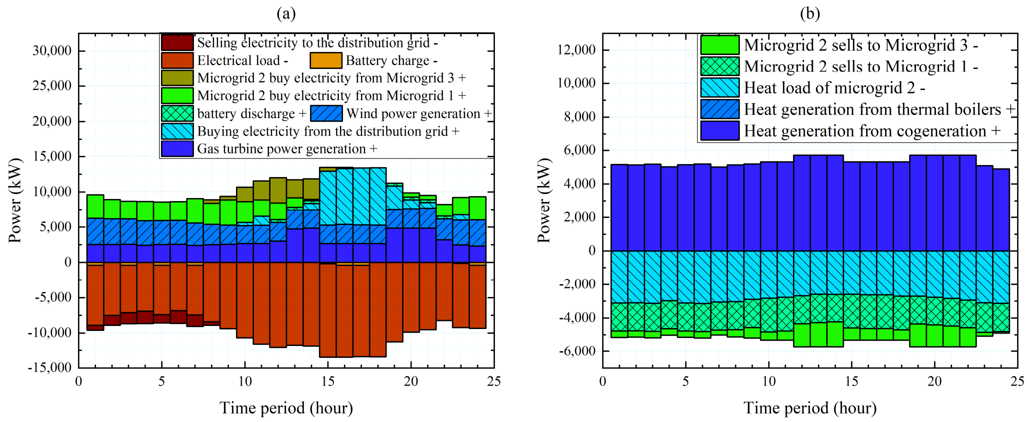

Figure 8. Post−alliance micro−grid 2 electric and heat balance results. (**a**) Electric balance results. (**b**) Heat balance results.

From the output of each device in Figure 8, it can be seen that the interaction between micro-grids can smooth the time-space contradiction between the source and load. After heat sharing is introduced on the basis of power sharing, the cogeneration of heat and power in micro-grid ② can run at a better heat-to-electricity ratio, achieving higher economies. At the same time, it avoids economic losses caused by low-power operation or even shutdown of cogeneration and increases the flexibility of the system.

5.4. Analysis of the Sub-Problem Q of the Reasonable Redistribution of the Benefits of the Multi-Micro-Grid Alliance Based on the Asymmetric Energy Mapping Function

The electric-thermal interaction quantity obtained in the above-mentioned alliance benefit maximization sub-problem is brought into the self-constructed asymmetric energy mapping contribution function that comprehensively considers the time period, energy type and supply and demand sides to obtain their respective contribution degrees, and then the further rational redistribution of the increased benefits of the multi-microgrid alliance. The results are shown in Appendix A.

It can be seen from Appendix A that after the electric heating double-layer sharing operation is completed, the operating cost of micro-grid ① is reduced from 28,835 CNY to 721 CNY, the operating cost of micro-grid ② is reduced from 63,055 CNY to 33,474 CNY and the operating cost of microgrid ③ has been reduced from 101,430 CNY to 88,199 CNY. Although all micro-grids are profitable, there is still the problem of uneven distribution. Therefore, the revenue of the three multi-microgrid subject coalitions is redistributed. Firstly, the electro-thermal interaction information of the electric heating double-layer sharing result is brought into the asymmetric energy mapping contribution function to obtain the contribution ratio of micro-grids ①,② and ③. Then, it is distributed to each microgrid subject according to the proportion of the contribution of each subject to realize the redistribution of benefits. In the end, the operating cost of micro-grid ① is reduced from 28,835 CNY to 1,079 CNY, the operating cost of micro-grid ② is reduced from 63,055 CNY to 30,770 CNY and the operating cost of micro-grid ③ is reduced from 101,430 CNY to 77,133 CNY. It shows that each micro-grid is paid according to work, and it proves that the necessity of time-sharing asymmetric benefit redistribution is more optimal.

5.5. Analysis of Carbon Emission Reduction Benefits of Electric Heating Double-Layer Sharing in Multi-Micro-Grid Alliance

Table A4 in Appendix A is the carbon emission reduction benefit analysis table of the electric and heat double-layer sharing of the multi-microgrid alliance, which shows the carbon emissions of the multi-micro-grid electricity and heat sharing before and after the alliance. The carbon emission of micro-grid ① is reduced from 86,159 kg to 85,628 kg, the carbon emission of micro-grid ② is reduced from 68,457 kg to 61,932 kg and the carbon emission of micro grid ③ is reduced from 91,240 kg to 90,335 kg. The electric heating double-layer sharing of the alliance is better than the electricity-only sharing, which can reduce the total carbon emission of the alliance from 237,895 kg to 211,803 kg. Although the carbon emission of micro-grid ② has a negative growth after energy sharing, the total carbon emission of the alliance is reduced from 245,856 kg to 211,803 kg, a decrease of 13.85%. Therefore, the multi-microgrid alliance of electric and heat double-layer sharing strategy based on the Nash game has the environmental benefit of reducing carbon emissions.

6. Conclusions

This paper proposes a multi-micro-grid electro-thermal double-layer sharing strategy based on the Nash game. The main conclusions are as follows:

(1) The electricity-thermal-gas-hydrogen-carbon coupling low-carbon transformation of the micro-grid structure is further carried out, and flue gas split carbon capture and P2G technology suitable for cogeneration are introduced, which reduce carbon emissions, carbon trading costs and operating costs when the micro-grid operates independently.

(2) The electric-thermal double-layer sharing strategy of multi-micro-grid based on the Nash game is constructed and solved by the ADMM algorithm, which improves the wind power consumption capacity of multi-micro-grids and reduces the total operating cost of the alliance.

(3) In order to further rationally redistribute the benefits of the multi-micro-grid alliance, an asymmetric energy mapping contribution function, by time period and energy type, is constructed to ensure that all individuals participating in the multi-micro-grid sharing of electricity and heat after the alliance benefit from double-layer sharing of the electricity and heat according to work.

Although the strategy in this paper has certain advantages, some aspects are still worthy of further improvement. For example, although the double-layer scheduling can further promote the consumption of abandoned wind and further promote the low-carbon economy, it can also avoid the problem that the ADMM algorithm is difficult to converge. However, the result of the lower-layer power sharing will limit the optimal heat-to-power ratio of the cogeneration unit when the upper-layer heat is shared and the CHP-to-electricity ratio is moved and optimized on the CHP power output contour line, which means the maximum electrothermal interaction potential of the system is still not fully exploited, requiring further research.

Author Contributions: Conceptualization, H.W. and C.W.; methodology, H.W.; software, H.W. and C.W.; validation, H.W., L.Z. and X.J.; formal analysis, H.W.; investigation, H.W.; resources, C.Y.; data curation, C.W.; writing-original draft preparation, H.W.; writing-review and editing, H.W. and C.W.; visualization, C.W.; supervision, H.W.; project administration, H.W.; funding acquisition, J.W. All authors have read and agreed to the published version of the manuscript.

Funding: This research received no external funding.

Data Availability Statement: Not applicable.

Acknowledgments: This work was supported by Jilin Province Science and Technology Department Project, China [20220101229JC].

Conflicts of Interest: The authors state no conflicts.

Appendix A

Table A1. Example parameters.

Reduced electric power proportional limit	0.05	The ideal unit heat production and gas consumption of the thermal boiler	9.7
Transferable electric power proportional limit	−0.1~0.1	The ratio of actual and ideal efficiency of thermal boiler	0.9
Transferable heat power proportional limit	−0.1~0.1	Carbon emissions per unit of heat produced by thermal boilers	0.65 kg
The initial charge of the battery	1000 kWh	Fan kWh carbon quota	0.424 kg/kWh
Battery charging efficiency	0.95	Thermal boiler carbon quota per unit of heat production	0.424 kg/kWh
Battery discharge efficiency	0.96	Carbon Capture Equipment Power Limits	1000 kW
Lower limit of battery charge	500 kWh	Power Limits for Electric-to-Gas Equipment	1000 kW
Upper limit of battery charge	2500 kWh	Cogeneration power supply upper limit	7000 kW
Battery charging power limit	0~300 kW	Cogeneration power supply lower limit	0 kW
Battery discharge power limit	0~300 kW	Thermoelectric Coupling Coefficient Kmin	0.15
Thermal power limit of thermal boiler	0~6500 kW	Thermoelectric Coupling Coefficient Kmax	0.2
Selling power limit	2000 kW	Thermoelectric Coupling Coefficient Kl	0.85
Buying Power Limit	10,000 kW	Cogeneration Ramp Constraint	1000 kW
Electric ratio of electric to gas operation	1.81	Heat transfer compensation unit price	0.016 CYN/kWh
Carbon Capture Operation Electric to Carbon Ratio	0.55	The maximum number of iterations	100
Electric to gas operation electric to carbon ratio	0.98	Alternating Direction Multiplier Method Convergence Accuracy	0.001
Unit cost of electrical interaction between micro-grids ① and ②	0.05 CNY/kWh	Carbon storage efficiency	0.97
Unit cost of electrical interaction between micro-grids ② and ③	0.15 CNY/kWh	Initial carbon charge	2000 kg
Unit cost of electrical interaction between micro-grids ① and ③	0.1 CNY/kWh	Carbon emission factor of cogeneration power generation	0.785 kg/kWh
Lagrange Multipliers	1×10^{-4}	Cogeneration heat carbon emission factor	0.15 kg/kWh
Unit cost of thermal interaction between micro-grids ① and ②	0.03 CNY/kWh	Unit price of natural gas	3.5 CNY/m^3
Unit cost of electrical interaction between micro-grids ② and ③	0.09 CNY/kWh	Unit price of electro-transfer compensation	0.3 CNY/kWh
Unit cost of electrical interaction between micro-grids ① and ③	0.06 CNY/kWh	Unit price of electricity reduction compensation	0.3 CNY/kWh

Table A2. Comparative analysis before and after the introduction of P2G in Micro-grid 2 for low-carbon transformation.

	P2G Consumption of CO_2 (kg)	Actual Carbon Emissions (kg)	Carbon Trading Cost (CNY)	Total Running Cost (CNY)
before remodeling	0	95,223	6176	64,717
after renovation	43,885	68,457	4248	63,055
Optimization amount	/	28.1%	31.2%	2.6%

Table A3. Reasonable redistribution results of multi-micro-grid alliance income.

Micro-Grid Number	Cost before Alliance (CNY)	Cost after Lower Electricity Sharing (CNY)	Cost after Upper Thermal Sharing (CNY)	Contribution	Redistribution of Benefits	Redistribution of Benefits (CNY)	Actual Running Cost after Alliance (CNY)
①	28,835	28,656	721	43,820	32.9%	27,756	1079
②	63,055	25,120	33,474	49,888	37.5%	32,285	30,770
③	101,430	101,864	88,199	39,176	29.6%	24,297	77,133
Total	193,320	155,641	122,395	132,984	100%	70,925	122,395

Table A4. Carbon emission reduction benefit analysis table of electric heating double-layer sharing in multi-micro-grid alliance.

Micro-Grid Number	Carbon Emissions before the Alliance (kg)	Carbon Emissions after Lower Electricity Sharing (kg)	Carbon Emissions after Upper Heat Sharing (kg)	Carbon Emission Reduction (kg)	Carbon Emission Reduction Rate (%)
①	86,159	85,628	58,894	27,265	31.64%
②	68,457	61,932	77,786	−9329	−13.63%
③	91,240	90,335	75,123	16,117	17.66%
Total	245,856	237,895	211,803	34,053	13.85%

References

1. Lin, B.; Li, Z. Towards world's low carbon development: The role of clean energy. *Appl. Energy* **2022**, *307*, 118160. [CrossRef]
2. Yan, Q.; Ai, X.; Li, J. Low-Carbon Economic Dispatch Based on a CCPP-P2G Virtual Power Plant Considering Carbon Trading and Green Certificates. *Sustainability* **2021**, *13*, 12423. [CrossRef]
3. Muqeet, H.A.; Javed, H.; Akhter, M.N.; Shahzad, M.; Munir, H.M.; Nadeem, M.U.; Bukhari, S.S.H.; Huba, M. Sustainable Solutions for Advanced Energy Management System of Campus Micro-grids: Model Opportunities and Future Challenges. *Sensors* **2022**, *22*, 2345. [CrossRef]
4. Han, L.; Morstyn, T.; McCulloch, M. Incentivizing prosumer coalitions with energy management using cooperative game theory. *IEEE Trans. Power Syst.* **2018**, *34*, 303–313. [CrossRef]
5. Hu, D.; Ye, Z.; Gao, Y.; Ye, Z.; Peng, Y.; Yu, N. Multi-agent Deep Reinforcement Learning for Voltage Control with Coordinated Active and Reactive Power Optimization. *IEEE Trans. Smart Grid* **2022**, *13*, 4873–4886. [CrossRef]
6. Xue, Z.; Pan, X.; Lv, Z.; Liu, T. Application of blockchain in energy and power business. In Proceedings of the 2020 4th International Conference on Electrical, Automation and Mechanical Engineering, Beijing, China, 21–22 June 2020; IOP Publishing: Bristol, UK, 2020; Volume 1626, p. 012057.
7. Zhang, Z.; Du, J.; Fedorovich, K.S.; Li, M.; Guo, J.; Xu, Z. Optimization strategy for power sharing and low-carbon operation of multi-micro-grid IES based on asymmetric nash bargaining. *Energy Strategy Rev.* **2022**, *44*, 100981. [CrossRef]
8. Wang, Y.; Wang, X.; Shao, C.; Gong, N. Distributed energy trading for an integrated energy system and electric vehicle charging stations: A Nash bargaining game approach. *Renew. Energy* **2020**, *155*, 513–530. [CrossRef]
9. Al-Saffar, M.; Musilek, P. Distributed optimization for distribution grids with stochastic der using multi-agent deep reinforcement learning. *IEEE Access* **2021**, *9*, 63059–63072. [CrossRef]
10. Chen, W.; Xiang, Y.; Liu, J. Optimal operation of virtual power plants with shared energy storage. *IET Smart Grid* **2022**. [CrossRef]
11. Li, L.; Shen, Y.; Ma, T. Research on daily energy trading strategy of multi-micro-grid on distribution side. In *IOP Conference Series: Earth and Environmental Science, Proceedings of the Fourth International Conference on Energy Engineering and Environmental Protection, Xiamen, China, 19–21 November 2019*; IOP Publishing: Bristol, UK, 2020; Volume 467, p. 012203.
12. Park, S.; Lee, J.; Bae, S.; Hwang, G.; Choi, J.K. Contribution-based energy-trading mechanism in micro-grids for future smart grid: A game theoretic approach. *IEEE Trans. Ind. Electron.* **2016**, *63*, 4255–4265. [CrossRef]
13. Cao, S.; Zhang, H.; Cao, K.; Chen, M.; Wu, Y.; Zhou, S. Day-ahead economic optimal dispatch of micro-grid cluster considering shared energy storage system and P2P transaction. *Front. Energy Res.* **2021**, *9*, 645017. [CrossRef]
14. Lv, S.; Hui, W.; Meng, X.; Yang, C.; Wang, M. Optimal capacity configuration model of power-to-gas equipment in wind-solar sustainable energy systems based on a novel spatiotemporal clustering algorithm: A pathway towards sustainable development. *Renew. Energy* **2022**, *201*, 240–255. [CrossRef]
15. Navon, A.; Ben Yosef, G.; Machlev, R.; Shapira, S.; Roy Chowdhury, N.; Belikov, J.; Orda, A.; Levron, Y. Applications of game theory to design and operation of modern power systems: A comprehensive review. *Energies* **2020**, *13*, 3982. [CrossRef]
16. Lang, Y.; Xu, D.; Liu, S.; Hu, L. A Scheduling Model for Wind Power Consumption Considering Source-Charge Coordination of Combined Heat and Power System in Low-Carbon Environment. In *IOP Conference Series: Materials Science and Engineering, Proceedings of the 2019 International Conference on Electrical Engineering and Control Technologies (CEECT 2019), Singapore, 5–7 December 2019*; IOP Publishing: Bristol, UK, 2020; Volume 752, p. 012004.

17. Zhang, X.; Guo, X.; Zhang, X. Bidding modes for renewable energy considering electricity-carbon integrated market mechanism based on multi-agent hybrid game. *Energy* **2023**, *263*, 125616. [CrossRef]
18. Yan, M.; Shahidehpour, M.; Paaso, A.; Zhang, L.; Alabdulwahab, A.; Abusorrah, A. Distribution network-constrained optimization of peer-to-peer transactive energy trading among multi-micro-grids. *IEEE Trans. Smart Grid* **2020**, *12*, 1033–1047. [CrossRef]
19. Yang, X.; He, H.; Zhang, Y.; Chen, Y.; Weng, G. Interactive energy management for enhancing power balances in multi-micro-grids. *IEEE Trans. Smart Grid* **2019**, *10*, 6055–6069. [CrossRef]
20. Havrlík, M.; Libra, M.; Poulek, V.; Kouřím, P. Analysis of Output Signal Distortion of Galvanic Isolation Circuits for Monitoring the Mains Voltage Waveform. *Sensors* **2022**, *22*, 7769. [CrossRef] [PubMed]
21. Zhang, N.; Sun, Q.; Yang, L.; Li, Y. Event-triggered distributed hybrid control scheme for the integrated energy system. *IEEE Trans. Ind. Inform.* **2021**, *18*, 835–846. [CrossRef]
22. Xu, D.; Wu, Q.; Zhou, B.; Li, C.; Bai, L.; Huang, S. Distributed multi-energy operation of coupled electricity, heating, and natural gas networks. *IEEE Trans. Sustain. Energy* **2019**, *11*, 2457–2469. [CrossRef]
23. Huang, W.; Zhang, N.; Yang, J.; Wang, Y.; Kang, C. Optimal configuration planning of multi-energy systems considering distributed renewable energy. *IEEE Trans. Smart Grid* **2017**, *10*, 1452–1464. [CrossRef]
24. Li, Y.; Zhang, H.; Liang, X.; Huang, B. Event-triggered-based distributed cooperative energy management for multienergy systems. *IEEE Trans. Ind. Inform.* **2018**, *15*, 2008–2022. [CrossRef]